ELSEVIER

Coordination Chemistry Reviews
200–202 (2000) 687–715

COORDINATION CHEMISTRY REVIEWS

www.elsevier.com/locate/ccr

Transition metal hydrides as ligands☆

Alberto Albinati [a], Luigi M. Venanzi [b,*]

[a] *Istituto di Chimica Farmaceutica, Università di Milano, Viale Abruzzi 42, I-20131 Milan, Italy*
[b] *Laboratorium für Anorganische Chemie, ETH Zentrum, Universitätstrasse 6, CH-8092 Zurich, Switzerland*

Received 14 October 1999; accepted 7 January 2000

Contents

Abstract

The characterization of $[(PPh_3)_3IrH_3AgH_3Ir(PPh_3)_3](CF_3SO_3)$ is reviewed. The structural and spectroscopic properties of $[(tripod)MH_3M'H_3M(tripod)](CF_3SO_3)$ (tripod = CH_3C-

☆ This article is based on the 'Sacconi Lecture' given by L.M.V. at the University of Florence on February 27, 1997.

* Corresponding author. Tel.: +41-1-6322851; fax: +41-1-6321090.
E-mail address: venanzi@inorg.chem.ethz.ch (L.M. Venanzi).

PII: S0010-8545(00)00257-5

$(CH_2PPh_2)_3$, $CH_3C(CH_2AsPh_2)_3$; M = Rh, Ir; M′ = Cu(I), Ag(I), Au(I), Cd(II)) are also reviewed. It is pointed out that (a) in the Cu(I) and Ag(I) species, each trihydride forms one stronger and one weaker M–H–M′–H–M interaction, (b) in the Au(I) species the trimetallic units are held together mainly by M–Au–M bonds and (c) in the Cd(II) species this cation may weakly interact with all six hydrides. Qualitative bonding schemes describing the M–H–M′–H–M interactions are presented. The formation and properties of the hydrido-bridged heterobimetallic complexes of the type $[(tripod)MH_3M'L_n](CF_3SO_3)$ (tripod = as above; M = Rh, Ir; M′ = Cu(I), Ag(I), Au(I), L = PR_3) are summarized. The structural features of the hexametallic complexes $[\{(CH_3C(CH_2PPh_2)_3)MH_3M'\}_3](CF_3SO_3)_3$ (M = Rh, Ir; M′ = Cu(I), Ag(I), Au(I)) are reviewed.

Keywords: Hydrido-bridged complexes; Bi-, tri-, and hexametallic complexes

1. Introduction

It is now well-established that mononuclear transition metal hydrides have a strong tendency to form di- or polynuclear assemblies containing M–H–M structural units [1] and much work has been carried out to identify the compounds formed [1], their structures [2], their spectroscopic characterization [3] and bonding properties [4].

Among the many types of compounds containing bridging hydrides, the binuclear complexes of the type $\{L_mH_xM(\mu\text{-}H)_yM'H_zL'_n\}$ have received particular attention as, in these compounds, the number of bridging hydrides ranges from one to four. Examples of complexes of these types are $[(CO)_5Cr(\mu\text{-}H)Cr(CO)_5)]^-$ (**1**) [5], $[(PEt_3)_2H_2Ir(\mu\text{-}H)_2Pt(PEt_3)_2]^+$ (**2**) [6], $[(PMe_3)_3Ru(\mu\text{-}H)_3Ru(PMe_3)_3]^+$ (**3**) [7] and $[(PEt_2Ph)_2H_2Re(\mu\text{-}H)_4ReH_2(PEt_2Ph)_2]$ (**4**) [8] whose structures are shown schematically below.

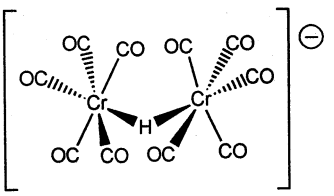

1

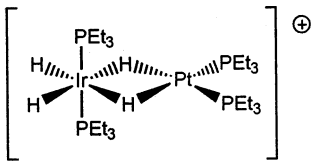

2

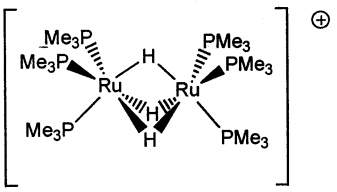

3

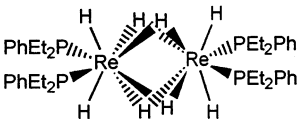

4

The M–H–M bridges are generally quite strong, exceptions made for those in some of the compounds containing only one bridging unit. The strength of an M–H–M bridge can be qualitatively assessed by the change of the M–H stretching vibration which occurs when the mononuclear complex $[MH_mL_n]$ forms the corresponding dinuclear species $[L_nH_{(m-x)}M(\mu\text{-}H)_xM'L'_n]$. Thus, the ν(W–H) vibration in $[WH_2(\eta^5\text{-}C_5H_5)_2]$ (**5**) is 1896 cm^{-1} [9] while ν(W–H–Pt) in $[(\eta^5\text{-}C_5H_5)_2HW(\mu\text{-}H)PtPh(PEt_3)_2][BF_4]$ (**6**) occurs at 1635 cm^{-1} (the terminal ν(W–H) in this compound is found at 1918 cm^{-1}) [10].

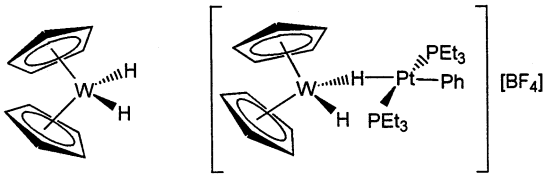

5 **6**

However, bridging interactions can be very strong even in complexes with a single M–H–M unit, as found in $[(PMe_3)_2(C_6F_5)Pt(\mu\text{-}H)Pt(C_6F_5)(PMe_3)_2](CF_3SO_3)$ (**7**): in this compound, $\nu(Pt\text{–}H)_{symm}$ and $\nu(Pt\text{–}H)_{asymm}$ occur at 1260 and 1020 cm^{-1}, respectively, while ν(Pt–H) in *trans*-$[PhH(C_6F_5)(PMe_3)_2]$ (**8**) it is found at 2060 cm^{-1} [11].

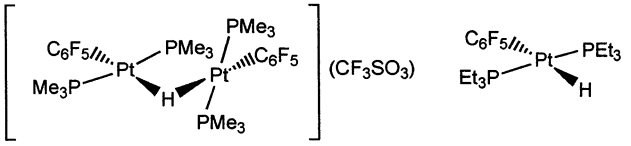

7 **8**

Such large shifts can pose problems with the identification of the M–H–M′ vibrations. However, recording the inelastic incoherent neutron scattering (IINS) spectrum[1] of the compound of interest can solve this problem. An example of such a spectrum, that of complex **7**, is shown in Fig. 1 (top trace).

[1] Thermal neutrons are very useful probes to study condensed matter as they can be used to study vibrational modes because their energy is comparable to that of molecular and lattice vibrations. IINS spectroscopy most closely resembles Raman scattering of light. In the experiment an incident neutron beam of known energy is scattered by the sample. A detector will then record the energy spectrum of the inelastically scattered neutrons. An advantage of this technique is that the inelastically scattered intensity depends on the incoherent scattering cross-section of each atom, which for hydrogen, is an order of magnitude greater than all other elements. Thus, vibrational modes involving hydrogen would be more prominent in this spectrum, see [12].

A problem may arise in the study of the hydrido-complexes of metals in order to distinguish the M–H vibrational modes from all other vibrations involving the H atoms of the ligands. In these cases a 'sample difference' technique may be used. The method is based on the large difference between the b_{inc} of H and D (79.91(4) and 2.04(3) barn, respectively). Thus the difference between two experimental IINS spectra of compounds containing a 'M–D' and a 'M–H' moiety respectively, should only leave the peaks involving the motion of the hydrides, provided that coupling of hydride motion to other modes is negligible (cf. [11]). Thus it is not necessary to fully deuterate the ligands.

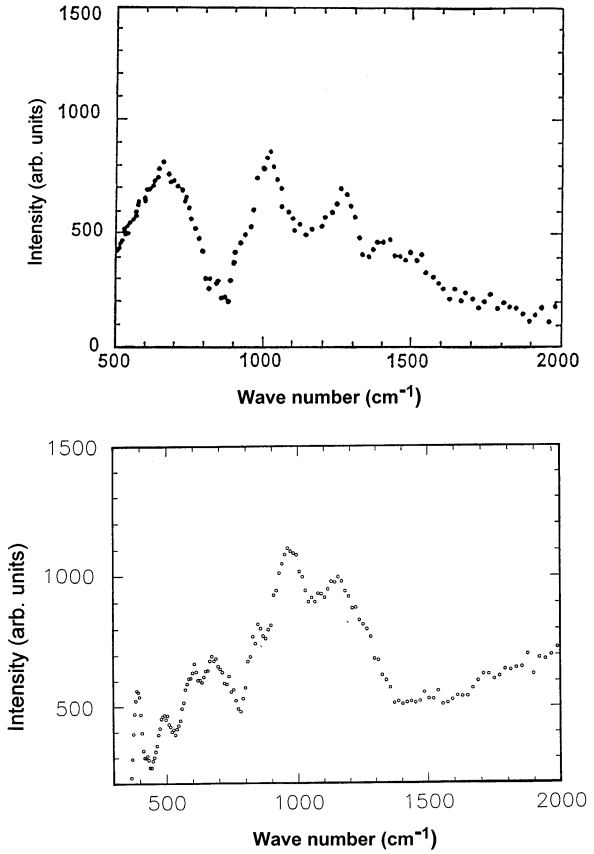

Fig. 1. The 'sample difference' inelastic incoherent neutron scattering spectrum of (a) $[(PMe_3)_2(C_6F_5)$-$Pt(\mu\text{-}H)Pt(C_6F_5)(PMe_3)_2](CF_3SO_3)$ (**7**) (top trace) and $[(PPh_3)_3HIr(\mu\text{-}H)_2Ag(\mu\text{-}H)_2IrH(PPh_3)_3](CF_3SO_3)$ (**10**) (bottom trace).

2. Trimetallic compounds

Much can be learned about M–H–M′ interactions by studying the structural changes that occur in a group of closely related compounds. One class of such compounds, which has received considerable attention in recent years, is that formed by reacting mononuclear polyhydrides of the type $[MH_m(PR_3)_n]$ with the coinage metal salts. Many of the resulting compounds are trimetallic and contain two transition metal atoms, M, and one coinage metal atom, M′. Early examples of such compounds are: $[\{(PMe_2Ph)_3ReH_5\}_2Cu][PF_6]$ (**9**) [13], $[\{(PPh_3)_3IrH_3\}_2Ag]$-(CF_3SO_3) (**10**) [14] and $[\{(PMe_2Ph)_3IrH_3\}_2Cu][PF_6]$ (**11**) [15]. As the rhodium $[RhH_3(PR_3)_3]$ and iridium $[IrH_3(PR_3)_3]$ trihydrides form the most extensive set compounds obtained to date, only the bridging hydrides formed by these two complexes will be discussed here.

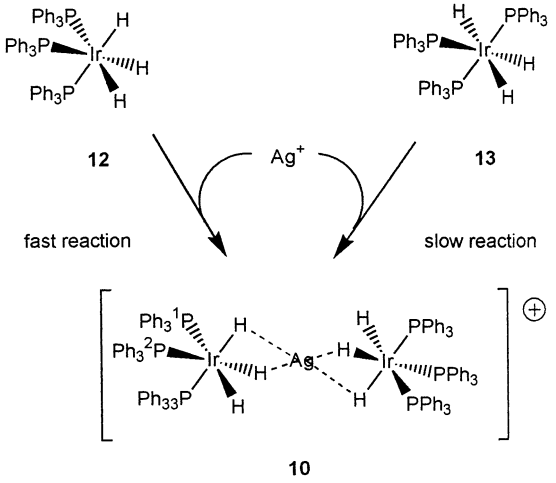

Scheme 1.

2.1. *[(PPh$_3$)$_3$IrH$_3$AgH$_3$Ir(PPh$_3$)$_3$](CF$_3$SO$_3$)*

One of the earliest reactions carried out using these hydrides is that of *fac*- and *mer*-[IrH$_3$(PPh$_3$)$_3$] (**12** and **13**, respectively) [16] with Ag^+ ions [14] (see Scheme 1). As can be seen there, *fac*-[IrH$_3$(PPh$_3$)$_3$] (**13**) rapidly reacts with Ag(CF$_3$SO$_3$) forming the trimetallic compound [(PPh$_3$)$_3$IrH$_3$AgH$_3$Ir(PPh$_3$)$_3$](CF$_3$SO$_3$) (**10**) [17]. This is a rather remarkable compound, as the addition of I^- to its solution does not cause the precipitation of AgI. The Ag^+ ion can only be removed from this complex by adding S^{2-} [17].

The X-ray crystal structure of [(PPh$_3$)$_3$IrH$_3$AgH$_3$Ir(PPh$_3$)$_3$](CF$_3$SO$_3$) (**10**) [18] was recently re-determined at $-90°C$[2] [19] in an attempt to locate the hydride ligands. Regrettably, this was not possible probably because of the strong disorder of the CF$_3$SO$_3$-counterions. An ORTEP view of one the two independent cations [19] in is shown in Fig. 2. As is apparent there, the silver ion is completely shielded by the phenyl groups of the phosphines (see also Section 2.3). Thus, the failure of the silver ion in this cation to react with iodide may be of steric origin.

The above study of complex **10**, raises two fundamental structural points, i.e. location of the hydrides and whether these ligands are bridging to the heterometal or not. Such structural assignments require neutron diffraction studies as X-ray data seldom allow the reliable location of these ligands on a Fourier map. Although an energy minimization procedure (HYDEX) has often been used for the calculation of hydride positions in transition metal complexes [20], this method often gives unacceptable results [21].

[2] The crystals are monoclinic, space group $P2_1/n$ with $a = 14.3628(2)$, $b = 30.8283$, $c = 24.1604(4)$ Å, $\beta = 91.527(1)°$, $R = 0.057$ (for 11 339 data with $F_o > 4.0\sigma(F)$. There are two independent half-molecules in the unit cell as each Ag atom lies in an inversion center.

In the absence of reliable structural data, the approximate hydride positions in these complexes are probably best inferred from the positions of the other donor atoms in the coordination polyhedron. A useful approach to the positioning of a bridging hydride in an M–H–M′ fragment is one in which one sets (a) the *trans*-L–M–H bond angle as 180° and (b) the M–H distance in the hydrido-bridged complex as being equal to that in related bridging hydrides [2b]. Obviously, the parameters thus obtained are not very accurate as in an M–H–M′ fragment (a) the *trans*-L–M–H bond angle is usually $< 180°$ and (b) the actual M–H distance may differ from the standard value used for the calculation [2b]. However, these effects are unlikely to change the qualitative conclusions reached.

Although the Ag atom in **10** is placed on a center of symmetry and, therefore, the Ir–Ag–Ir angle is 180°, the two *fac*-[$IrH_3(PPh_3)_3$] octahedra are symmetrically twisted with respect to this central atom. This is clearly shown by the Ag–P distances. These are: Ag–P1 = 4.383(4), Ag–P2 = 4.114(4) and Ag–P3 = 4.101(4) Å. Thus, the above 'geometrical construction' model gives the following calculated values: $Ag–H1_{trans\text{-}P1} = 2.5$, $Ag–H2_{trans\text{-}P2} = 2.2$ and $Ag–H3_{trans\text{-}P3} = 1.9$ Å. One can then conclude that, in this complex, there are two significant Ir–H–Ag-interactions — those with H3 and H3′, and two weaker ones — those with H2 and H2′. The Ag–H1 and Ag–H1′ distances are very long and, therefore, the Ir–H1 and IrH1′ bonds are to be considered as terminal.

Valuable qualitative information about the Ir–H–Ag interactions in [$(PPh_3)_3HIr(\mu\text{-}H)_2Ag(\mu\text{-}H)_2IrH(PPh_3)_3$]($CF_3SO_3$) (**10**) is also provided by its IR

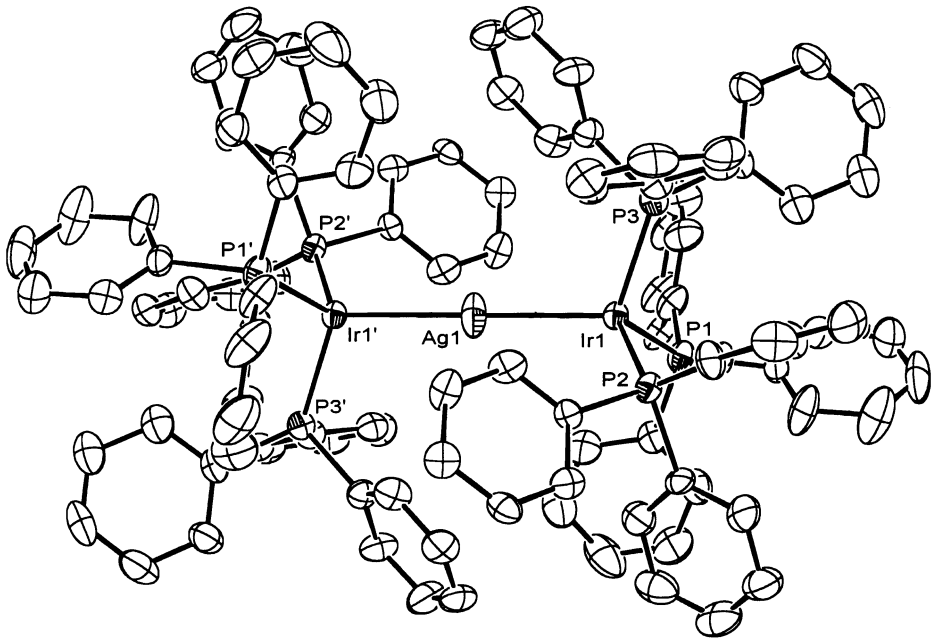

Fig. 2. An ORTEP view of the cation in [$(PPh_3)_3HIr(\mu\text{-}H)_2Ag(\mu\text{-}H)_2IrH(PPh_3)_3$]($CF_3SO_3$) (**10**).

spectrum in the hydride region. To avoid complications with the vibrations due to the aromatic C–H bonds, the IR spectra of *fac*-$[IrH_3\{P(C_6D_5)_3\}_3]$ (**12^D**) and $[\{P(C_6D_5)_3\}_3HIr(\mu\text{-}H)_2Ag(\mu\text{-}H)_2IrH\{P(C_6D_5)_3\}_3](CF_3SO_3)$ (**10^D**) were recorded. The bands in the hydride region, of these two compounds [22] are shown in Fig. 3. The ν(Ir–H) vibrations in the spectrum of **12^D** show up as a double band with a maximum at 2080 cm^{-1} while the corresponding absorptions in **10^D** appear as a

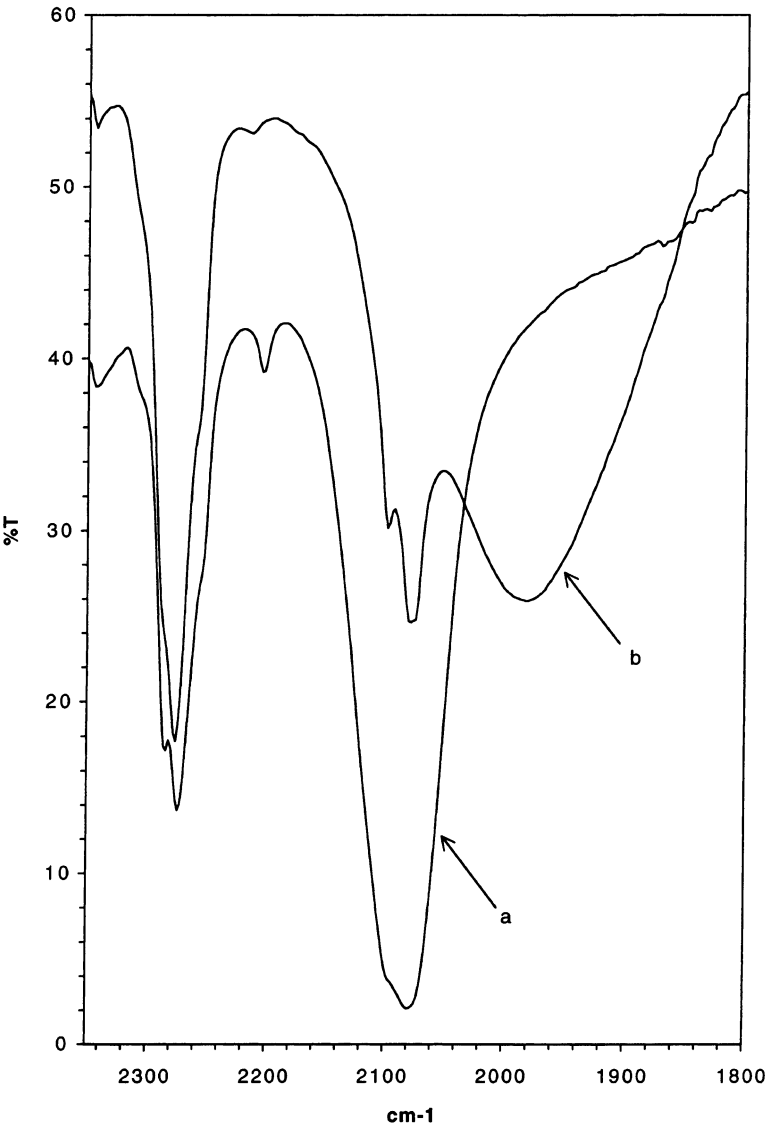

Fig. 3. The IR spectra, in the hydride region, of *fac*-$[IrH_3\{P(C_6D_5)_3\}_3]$ (**12^D**) (trace (a)) and $[\{P(C_6D_5)_3\}_3HIr(\mu\text{-}H)_2Ag(\mu\text{-}H)_2IrH\{P(C_6D_5)_3\}_3](CF_3SO_3)$ (**10^D**) (trace (b)).

broad band at 1976 and a narrower band at 2079 cm^{-1}. Thus, also this spectroscopic study indicates that, in this trimetallic complex, some of the Ir–H bonds are terminal. It is noteworthy that, in this case, $\Delta\nu$ is only 100 cm^{-1}. This small difference may indicate that, although significant, the bridging interactions in this compound are rather weak.

More information about complex **10** is provided by its IINS spectrum (see Fig. 1 (bottom trace)) [23]. In this spectrum the terminal stretches are not observable due to the low resolution in this region of the instrument used [24]. However, one can see two strong bands at ca. 1250 and 1050 cm^{-1}, which are diagnostic of a μ^2-bridge [25].

Structural information in solution is provided by the NMR spectra of **10**. Thus, the ^{109}Ag–^{31}P correlation spectra shown in Fig. 4 [26] clearly show that there is a significant coupling between the hydrides and the silver ion ($^1J(^{107}Ag,^{31}P) = 48$, $^1J(^{109}Ag,^{31}P) = 56$, $^2J(^{107,109}Ag,^{31}P) = 20$ Hz).

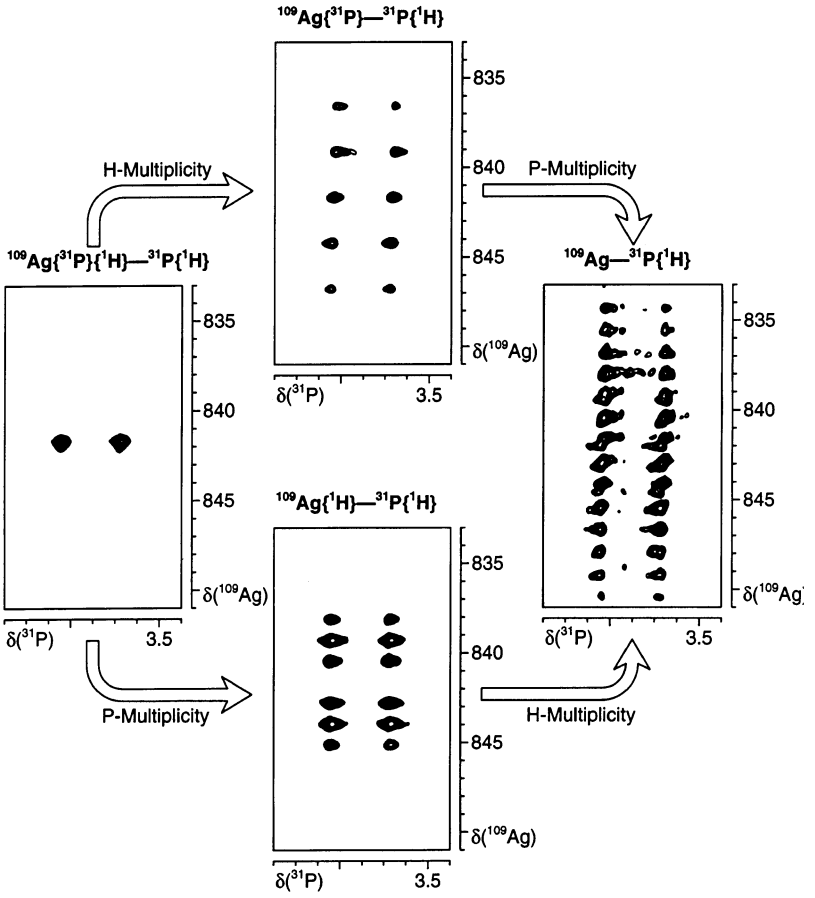

Fig. 4. The ^{109}Ag–^{31}P correlation spectra of $[(PPh_3)_3HIr(\mu\text{-}H)_2Ag(\mu\text{-}H)_2IrH(PPh_3)_3](CF_3SO_3)$ (**10**).

2.2. Complexes of the type $[(tripod)MH_3M'H_3M(tripod)](CF_3SO_3)$

Compounds related to the PPh_3 complex (**10**) are obtained when the tripodal ligands triphos and triars are used as co-ligands, i.e. $[(tripod)MH_3M'H_3M(tripod)]^+$ (tripod = triphos, M = Rh, Ir; M′ = Cu(I), Ag(I) and Au(I) ($\mathbf{14_{MM'M}}$); tripod = triars ($CH_3C(CH_2AsPh_2)_3$); M = Rh, Ir; M′ = Cu(I), Ag(I) and Au(I) ($\mathbf{15_{MM'M}}$)) [27].

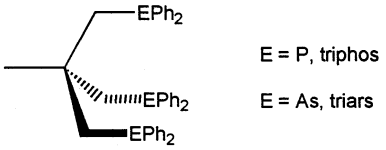

Their formation is remarkably easy: it suffices to mix, at room temperature, solutions containing the appropriate ratios of the mononuclear hydrides $[RhH_3(triphos)]$ (**16**) [28], $[RhH_3(triars)]$ (**17**) [27]; $[IrH_3(triphos)]$ (**18**) [29] or $[IrH_3(triars)]$ (**19**)) [17] with $Cu(CF_3SO_3)\cdot 1/2C_6H_6$ for M′ = Cu(I), with $Ag(CF_3SO_3)$ for M′ = Ag(I) and with $[AuBr_2]^-$, followed by $Ag(CF_3SO_3)$, for Au(I) (see Scheme 2) [27].

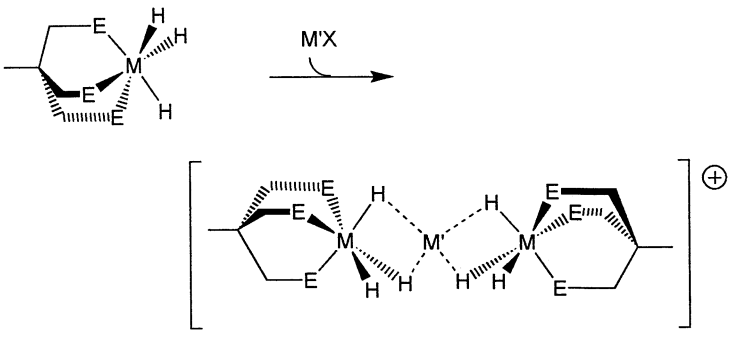

(E = P ($\mathbf{14_{MM'M}}$), As ($\mathbf{15_{MM'M}}$); M = Rh, Ir;

M'X = $Cu(CF_3SO_3).1/2C_6H_6$, $Ag(CF_3SO_3)$, $[AuBr_2]^-$)

Scheme 2.

2.2.1. Copper(I) and silver(I) complexes

The X-ray crystal structures of several complexes of this type were determined, i.e. $[(triphos)RhH_3AgH_3Rh(triphos)](CF_3SO_3)$ ($\mathbf{14_{RhAgRh}}$) [30], $[(triphos)RhH_3CuH_3Rh(triphos)](CF_3SO_3)$ ($\mathbf{14_{RhCuRh}}$) [30], $[(triphos)IrH_3AgH_3Ir(triphos)](CF_3SO_3)$ ($\mathbf{14_{IrAgIr}}$) [31] and $[(triphos)IrH_3AuH_3Ir(triphos)](CF_3SO_3)$ ($\mathbf{14_{IrAuIr}}$) [31]. An ORTEP view of the cation in $[(triphos)IrH_3AgH_3Ir(triphos)](CF_3SO_3)$ ($\mathbf{14_{IrAgIr}}$) is shown in Fig. 5. Interestingly, the Ir–Ag–Ir angle in this compound is 170.8(1)° and *not* 180°, as found in $[(PPh_3)_3IrH_3AgH_3Ir(PPh_3)_3](CF_3SO_3)$ (**10**). This structural feature is common to all the copper and silver compounds mentioned above.

The P–Ag distances in $\mathbf{14_{IrAgIr}}$ (Ag–P1 = 4.133(5), Ag–P2 = 4.572(4) and Ag–P3 = 4.582(4) Å) indicate that *only two* hydrides of each 'MH_3(triphos)'-moiety interact with the Ag^+ ion. Using the 'geometrical construction' model, one obtains the following calculated Ag–H distances: Ag–$H1_{trans\text{-}P1}$ = 1.9, Ag–$H2_{trans\text{-}P2}$ = 2.7 and Ag–$H3_{trans\text{-}P3}$ = 2.1 Å.

Confirmation of the presence of *terminal* M–H bonds in these compounds is provided by their IR spectra in the hydride region. Thus, the IR spectrum of [(triphos)HIr(μ-H)$_2$Ag(μ$_2$-H)IrH(triphos)](CF$_3$SO$_3$) ($\mathbf{14_{IrAgIr}}$) [27] (see Fig. 6 (trace (b)) shows one fairly narrow band at ca. 2020 cm^{-1}, i.e. a value characteristic for the terminal Ir–H bonds in [IrH_3(triphos)] (**18**) (see Fig. 6, trace (a)) and a broad band centered at ca. 1850 cm^{-1}. This spectrum is common to all the copper and silver, triphos- ($\mathbf{14_{MM'M}}$, M = Rh, Ir; M′ = Cu, Ag) and triars-containing ($\mathbf{15_{MM'M}}$, M = Rh, Ir; M′ = Cu, Ag) complexes of this type *both in solution and in the solid state* [27]. Thus, the non-linearity of the M–M′–M unit and the presence of both terminal (M–H) and bridging (M–H–M′) bonds are not due to packing effects.

2.2.2. Gold(I) complexes

Surprisingly, the gold(I) complexes [(triphos)IrH_3AuH_3Ir(triphos)](CF$_3$SO$_3$) ($\mathbf{14_{MAuM}}$, M = Rh, Ir) and [(triars)IrH_3AuH_3Ir(triars)](CF$_3$SO$_3$) ($\mathbf{15_{MAuM}}$, M = Rh,

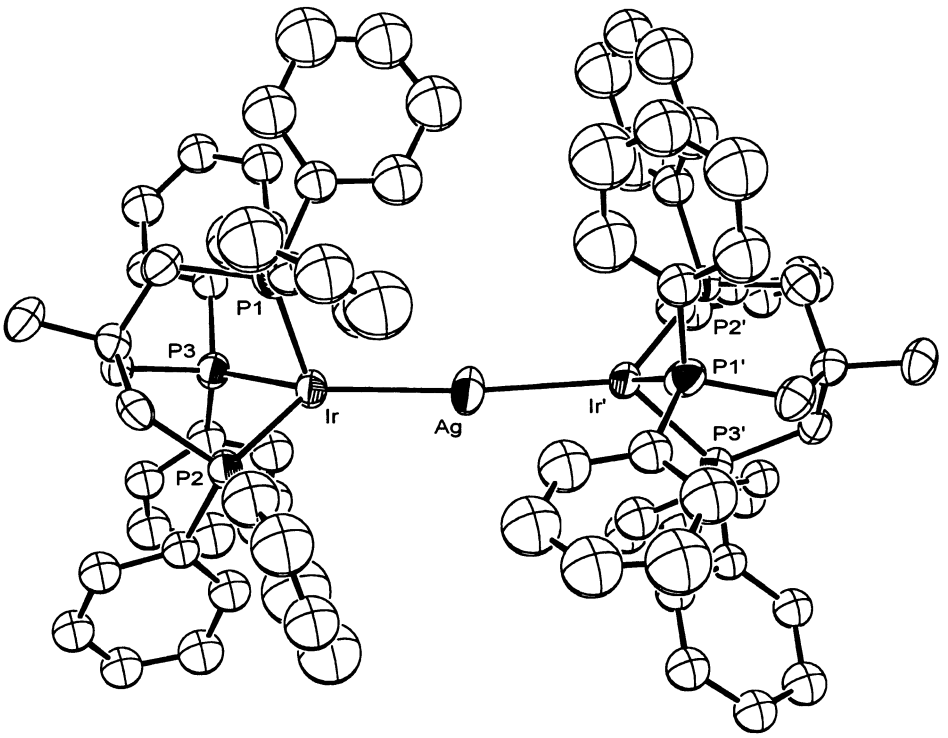

Fig. 5. An ORTEP view of the cation in [(triphos)HIr(μ-H)$_2$Ag(μ-H)$_2$IrH(triphos)](CF$_3$SO$_3$) ($\mathbf{14_{IrAgIr}}$).

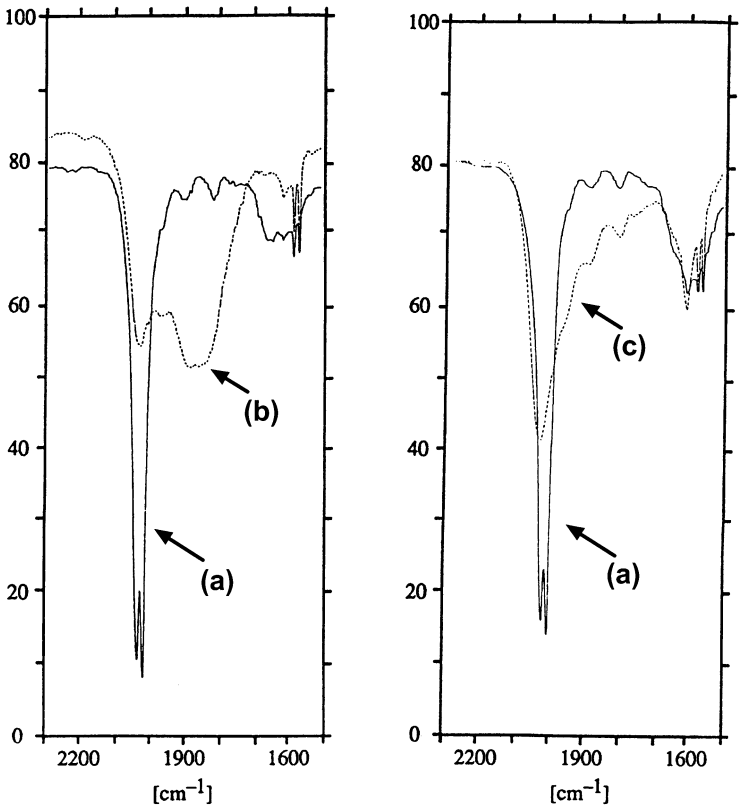

Fig. 6. The IR spectra, in the hydride region, of $[IrH_3(triphos)_3]$ (**18**) (trace (a)), $[(triphos)HIr(\mu\text{-}H)_2Ag(\mu\text{-}H)_2IrH(triphos)](CF_3SO_3)$ ($\mathbf{14_{IrAgIr}}$) (trace (b)) and $[(triphos)H_3IrAuIrH_3(triphos)](CF_3SO_3)$ ($\mathbf{14_{IrAuIr}}$) (trace (c)). (The low-energy bands between 1800 and 1950 cm^{-1} are due to C–H vibrations).

Ir) differ from their copper and silver analogs. This is immediately apparent from their IR spectra (see Fig. 6, trace (c) for that of $\mathbf{14_{IrAuIr}}$) [27]. These do not show bands in the region of the bridging hydrides analogous of those of the corresponding copper ($\mathbf{14_{MCuM}}$ or $\mathbf{15_{MCuM}}$; M = Rh, Ir) and silver complexes ($\mathbf{14_{MAgM}}$ or $\mathbf{15_{MAgM}}$; M = Rh, Ir) (see Fig. 6). They only show a shoulder on the low-energy side of the main band at ca. 1978 cm^{-1}. Thus, in the gold complexes the trimetallic units may be held together mainly by metal–metal bonds.

The X-ray crystal structure of $[(triphos)IrH_3AuH_3Ir(triphos)](CF_3SO_3)$ ($\mathbf{14_{IrAuIr}}$) [30] (see Fig. 7) shows that the cation retains many of the geometric features of the corresponding copper and silver compounds, e.g. the bent Ir–Au–Ir moiety (170.3(1)°). However, in this compound the Ir–Au distances *are slightly different*, i.e. Ir1–Au = 2.7165(8) and Ir2–Au2 = 2.6919(3) Å. This difference is also observed in the P–Au (average) distances as P(1,2,3)–Au is 4.468(4) while P(4,5,6)–Au is

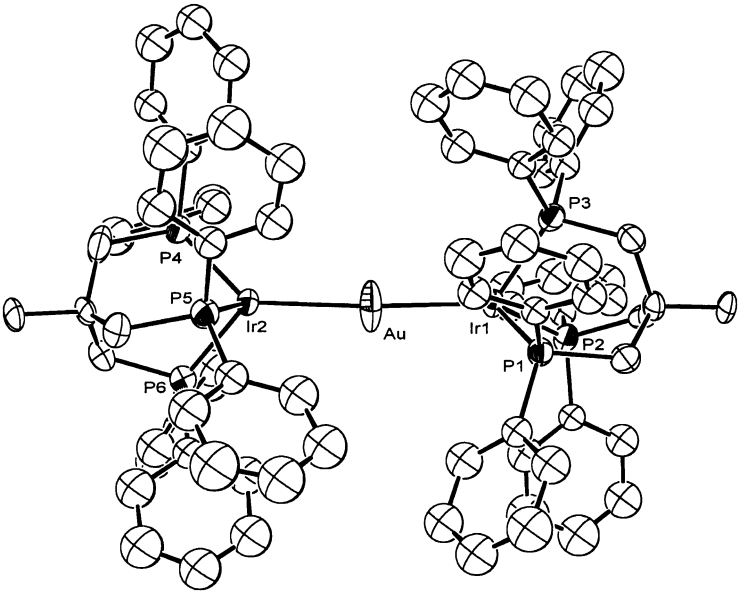

Fig. 7. An ORTEP view of the cation in $[(triphos)H_3IrAuIrH_3(triphos)](CF_3SO_3)$ ($\mathbf{14_{IrAuIr}}$).

4.399(4) Å. Interestingly, the calculated Au–H (average) distances are: Au–H1 = 1.7, Au–H2 = 2.8 and Au–H3 = 2.3 Å.

2.2.3. Cadmium(II) complexes

Also cadmium(II) forms the trimetallic complexes $[(tripod)MH_3CdH_3M(tripod)](CF_3SO_3)_2$ (M = Rh, Ir; tripod = triphos ($\mathbf{14_{MCdM}}$), triars ($\mathbf{15_{MCdM}}$). Even in these cases simple mixing of the components, in the appropriate ratios, gives the trimetallic compounds [27]. However, their IR spectra (see Fig. 8, trace (b)) show only one broad band in the hydride region [27]. Thus, it is likely that also in the compounds $\mathbf{14_{MCdM}}$ and $\mathbf{15_{MCdM}}$ all six hydrides are interacting, albeit weakly, with the cadmium atom.

2.2.4. Comparative data

The above trimetallic complexes $[L_3MH_3M'H_3ML_3](CF_3SO_3)_n$ are of four types:

1. The first type, the most common, found in $[(triphos)MH_3M'H_3M(triphos)](CF_3SO_3)$ ($\mathbf{14_{MM'M}}$) and $[(triars)MH_3M'H_3M(triars)](CF_3SO_3)$ ($\mathbf{15_{MM'M}}$) (M = Rh, Ir; M′ = Cu, Ag), features a slightly bent M–M′–M arrangement with four relatively weak M–H–M′ interactions and two terminal M–H bonds.
2. The second type is restricted to $[(PPh_3)_3IrH_3AgH_3Ir(PPh_3)_3](CF_3SO_3)$ (**10**) and shows a linear Ir–Ag–Ir arrangement, but also contains four fairly weak Ir–H–Ag interactions and two terminal M–H bonds.

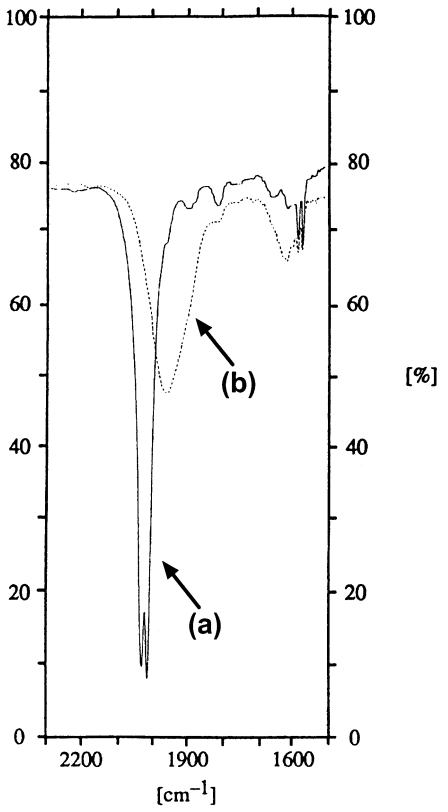

Fig. 8. The IR spectra, in the hydride region, of *fac*-[$IrH_3(PPh_3)_3$] (**18**) (trace (a)) and [(triphos)Ir(μ-H)$_3$Cd(μ-H)$_3$IrH(triphos)](CF$_3$SO$_3$)$_2$ (**14$_{IrCdIr}$**) (trace (b)).

3. The third type, found in the gold complexes [(triphos)MH_3AuH_3M-(triphos)](CF$_3$SO$_3$) (**14$_{MAuM}$**) and [(triars)$MH_3M'H_3M$(triars)](CF$_3$SO$_3$) (**15$_{MAuM}$**) (M = Rh, Ir) does not show significant Au–H interactions.
4. The last type, observed in [(triphos)MH_3CdH_3M(triphos)](CF$_3$SO$_3$)$_2$ (**14$_{MCdM}$**) and [(triars)MH_3CdH_3M(triars)](CF$_3$SO$_3$)$_2$ (**15$_{MCdM}$**) (M = Rh, Ir), may contain a linear M–M′–M arrangement with six weak, apparently equal, M–H–M′ interactions.

The observed P–M, P–M′ distances and the M–M′–M bond angles, as well as the calculated M′–H distances, are collected in Table 1.

2.3. Bonding scheme

A qualitative description of the bonding in the trimetallic complexes [$L_3MH_3M'H_3ML_3$] can be derived from that used for the bimetallic species [L_nM(μ-H)ML_n]. A pictorial representation of the orbital interactions in a single, *linear*

M–H–M′ bridge in $[(CO)_5Cr(\mu\text{-}H)Cr(CO)_5]^-$ (**1**) [32] is shown in Scheme 3 (for convenience, in this scheme the orbitals available for M–H–M bonding in the $\{Cr(CO)_5\}$-fragments are shown as the $3d_{z^2}$-orbitals). However, as practically all M–H–M moieties are *non-linear*, this feature has been rationalized [32] as shown in Scheme 4: the bending of the three-center, two-electron M–H–M moiety leads to an overall energy lowering.

Also the interaction within an 'MH_3–M′–H_3M'-fragment in complex **10** and those of type $\mathbf{14_{MM'M}}$ can be qualitatively described using the model outlined above envisaging that each trihydride forms *only one* M–H–M′ bridge. However, the structural and spectroscopic evidence presented above, and earlier studies of related compounds containing trihydrides of the type $[MH_3(PR_3)_3]$ [2,3], indicates that more than one hydride from each MH_3 building block may interact with the coinage metal cation. Therefore, it is more convenient to start by constructing a set of 'equivalent orbitals' from the individual M–H bonds [32] as shown on the top

Table 1
Observed P–M, M–M′ and P–M′ (Å) distances and the M–M′–M bond angles (°), as well as the calculated H–M′ distances[a] (Å) in the trimetallic complexes $[(PPh_3)_3IrH_3AgH_3Ir(PPh_3)_3](CF_3SO_3)$ (**10**) and [(triphos)$MH_3M'H_3M$(triphos)](CF_3SO_3) (M = Rh, M′ = Cu ($\mathbf{14_{RhCuRh}}$), Ag ($\mathbf{14_{RhAgRh}}$); M = Ir, M′ = Ag ($\mathbf{14_{IrAgIr}}$), Au ($\mathbf{14_{IrAuIr}}$))

Complex	P–M	M–M′	P–M′	H–M′[a,b]	M–M′–M
10	2.354(3)	2.7122(4)	4.104(4)	1.9	180
	2.354(3)		4.111(4)	2.2	
	2.362(3)		4.383(4)	2.5	
$\mathbf{14_{RhCuRh}}$	2.29(1)	2.540(3)	4.12(1)	1.8	170.3(2)
	2.35(1)		4.42(1)	2.0	
	2.32(1)		4.38(3)	2.4	
$\mathbf{14_{RhAgRh}}$	2.290(7)	2.681(2)	4.529(8)	1.9	168.4(2)
	2.334(10)		4.507(9)	2.2	
	2.295(8)		4.186	2.6	
$\mathbf{14_{IrAgIr}}$	2.294(5)	2.7079(6)	4.133(5)	1.9	170.8(1)
	2.303(5)		4.571(4)	2.1	
	2.308(6)		4.582(4)	2.7	
$\mathbf{14_{IrAuIr}}$	2.231(4)[c]	2.7165(8)[e]	4.369(4)[c]	1.7[g]	170.31(4)
	2.297(3)[c]	2.6918(8)[f]	4.773(4)[c]	2.3[g]	
	2.336(4)[c]		3.992(4)[c]	2.8[g]	
	2.287(4)[d]		4.603(4)[d]		
	2.328(4)[d]		4.093(4)[d]		
	2.327(4)[d]		4.552(4)[d]		

[a] Calculated by assuming that M–H = 1.82 Å and *trans*-P–M–H = 180°.
[b] These data relate to one of the two independent molecules in the unit cell.
[c] P–Ir1.
[d] P–Ir2.
[e] Ir1–Au.
[f] Ir2–Au.
[g] Average values.

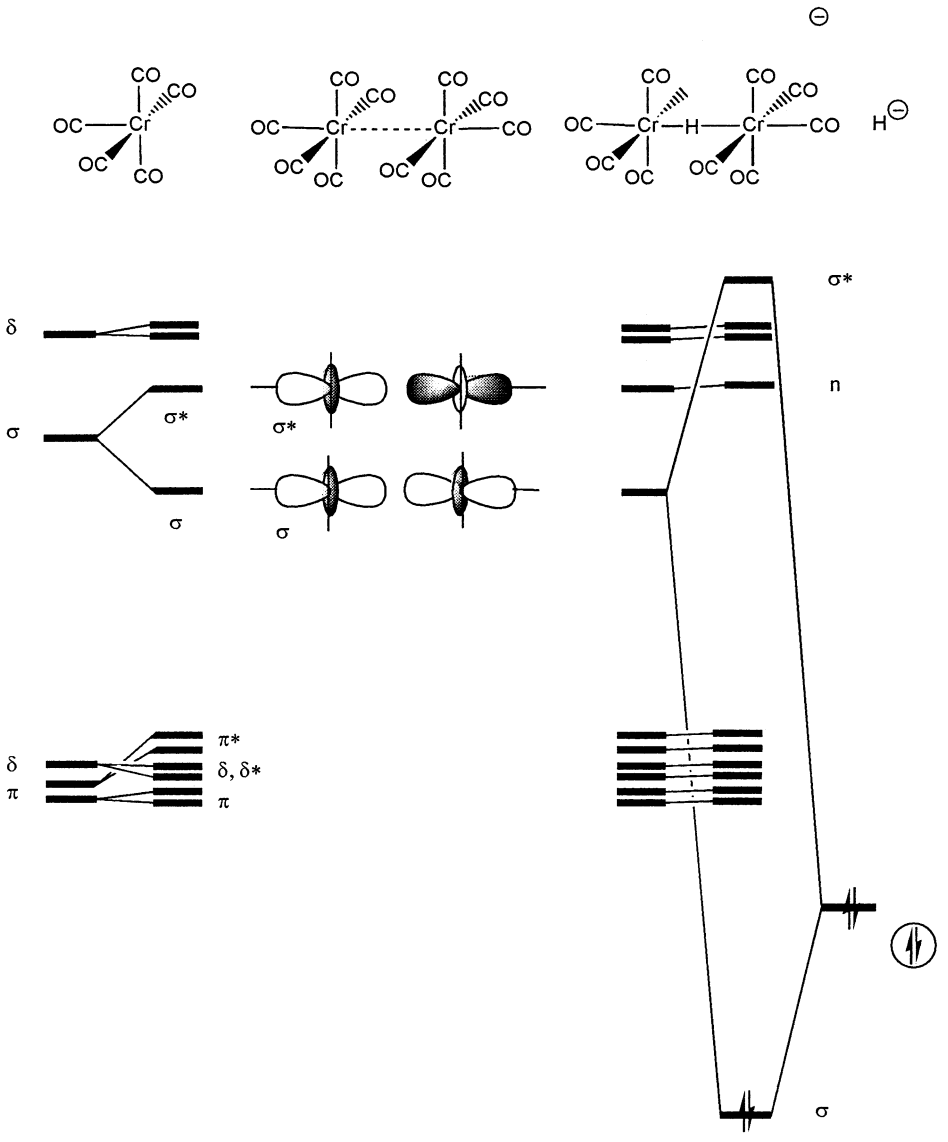

Scheme 3.

part of Scheme 5. As can be seen there, the linear combination of the σ-orbitals of the M–H bonds in *fac*-L_3MH_3 produces one a_1-type and one e-type orbital. It can then be envisaged that the main M–H–M′–H–M interaction occurs between the *n*s-orbital of M′ and the a_1-orbital of each trihydride fragment. A qualitative representation of the resulting σ-, *n*- and σ*-levels, for both linear and bent M–M′–M arrangements, are shown in the lower part of Scheme 5.

As the two a_1-orbitals are both doubly occupied while the $s_{M'}$-orbital is vacant, it is expected that the resulting lowest energy state of this 'four-electron three-center' system gives a linear of the M–M′–M arrangement [32], contrary to what observed in most of the compounds of type $\mathbf{14}_{\mathbf{MM'M}}$.

In order to produce a bent M–M′–M fragment, one can postulate that there are additional interactions between the three metal centers, e.g. between the vacant p_x and p_y orbitals (z being the main molecular axis) of M′ and the doubly occupied e-orbitals of the two trihydrides. Appropriate calculations will be required to establish the feasibility of such interactions.

The proposed bonding scheme apparently does not account for

1. the linear Ir–Ag–Ir arrangement present in $[(Ph_3P)_3IrH_3AgH_3Ir(PPh_3)_3](CF_3SO_3)$ (**10**);

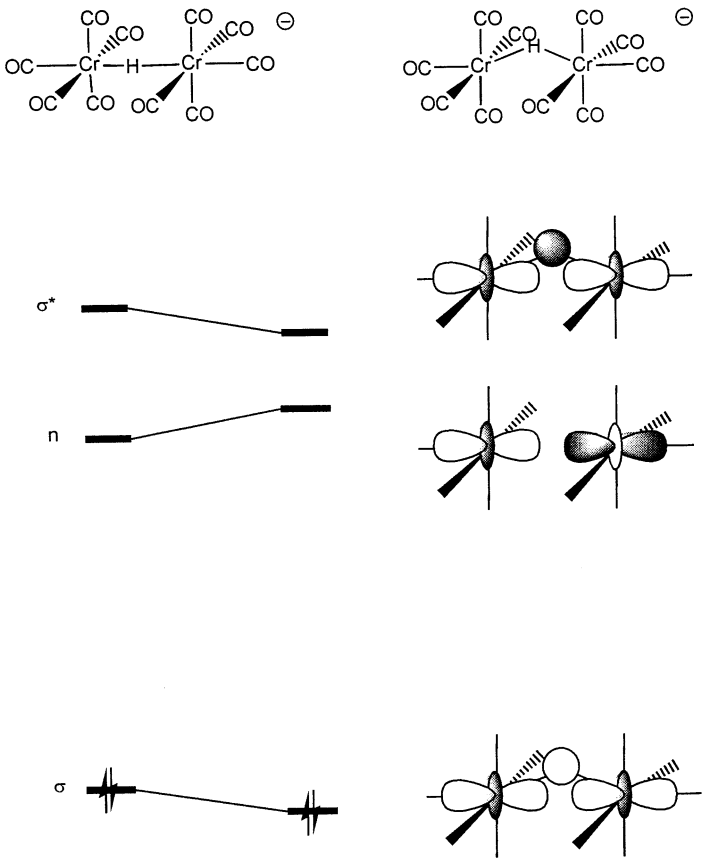

(The π, π*, δ and δ* orbitals have been omitted for simplicity)

Scheme 4.

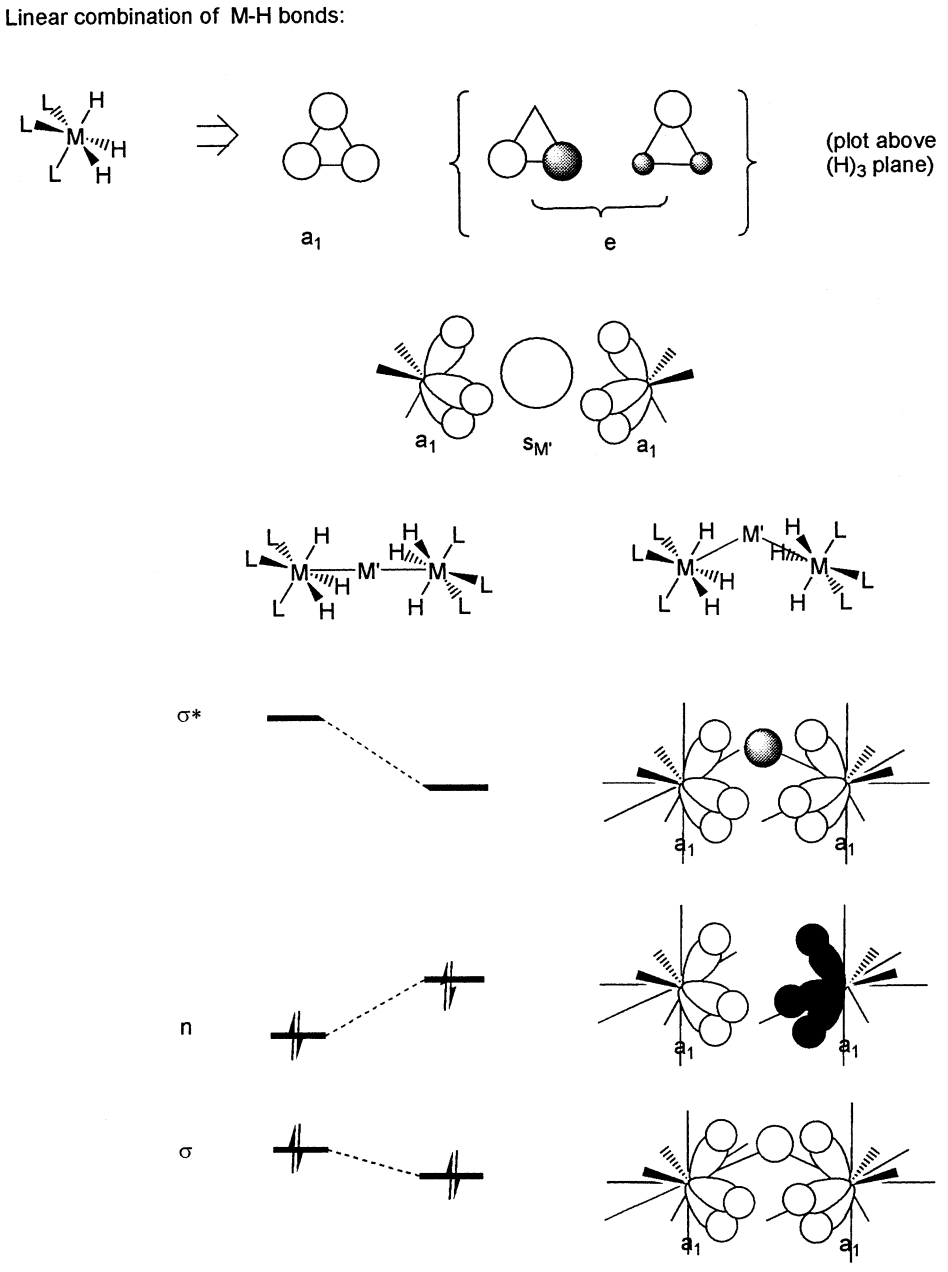

Scheme 5.

2. the interaction between all six hydrides with Cd^{2+} and the postulated linear M–Cd–M arrangement in $[(tripod)MH_3CdH_3M(tripod)](CF_3SO_3)_2$ (M = Rh, Ir; tripod = triphos (**14**$_{MCdM}$), triars (**15**$_{MCdM}$) and

3. the practical absence of Au–H interactions in the gold complexes [(triphos)IrH_3AuH_3Ir(triphos)](CF_3SO_3) (**14_{MAuM}**, M = Rh, Ir) and [(triars)-IrH_3AuH_3)Ir(triars)](CF_3SO_3) (**15_{MAuM}**, M = Rh, Ir).

In fact, these 'exceptions' do not invalidate the above bonding description. Thus, steric reasons may be responsible for the 180° Ir–Ag–Ir angle in the PPh_3-complex **10**. This can be visualized by comparing the space-filling models shown in Fig. 9. As can be seen there, in complex (**10**) (model (a), top) the van der Waals repulsions between the phenyl groups on either side of the coinage metal appear to force a linear Ir–Ag–Ir arrangement. However, the tendency of M′ to significantly interact with only two of the hydrides of each $[IrH_3(PPh_3)_3]$ unit is accommodated by twisting the two octahedra around the Ir–Ag–Ir axis. This effect is not present when the substituents on the phosphorus atoms are less bulky, as is the case of the triphos complexes, e.g. in **14_{IrAgIr}** (see model (b), middle).

The extent of the M–M′–M bending in complexes **$14_{MM'M}$** and **$15_{MM'M}$** *is unlikely* to be determined by steric repulsions between the phenyl substituents on the triphos ligands on each side of the M′-atom although the space-filling model (b) may indicate otherwise. This follows from the work of Caulton and co-workers [15]. They find that the Ir–Cu–Ir angle in $[(PMe_2Ph)_3IrH_3CuH_3Ir(PMe_2Ph)_3][PF_6]$ (**11**) is 176.0(2)° although there are no apparent steric reasons for such a wide angle (see model (c), bottom).

The bonding scheme outlined above also provides a rationalization for the proposed linearity of the M–Cd–M units in complexes **14_{MCdM}** and **15_{MCdM}**: While the $\Delta(E_{ns} - E_{np})$ values for Cu(I) and Ag(I) are 5.51 and 5.08 eV, respectively, that of Cd(II) is 6.62 eV [33]. Thus, the $d_M - p_{M'}$ interactions would be energetically unfavorable in the latter case. The overlap at the Cd-atom would involve only the 5s-orbitals of cadmium and, consequently, six very weak M–H–Cd–H–M interactions with a linear M–Cd–M fragment.

Finally, one must rationalize the observation that, in the gold complexes **14_{MAuM}** and **15_{MAuM}**, the M–H–M′ interactions are practically non-existent and yet the M–Au–M unit remains bent. Firstly, in these cases, the high stability of the trinuclear species may be connected with strong direct M–M′ interactions due to relativistic, spin-orbit and correlation effects [34]. The metal–metal overlap could occur between the $M(d_{xz})$- or $M(d_{xz})$-orbitals and the Au(6s) orbital. This would require a bent M–H–Au–H–M-arrangement, as shown schematically below.

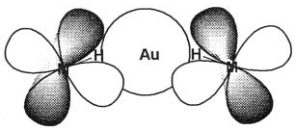

One can then conclude that complexes of the types **$14_{MM'M}$** and **$15_{MM'M}$** are best formed by metal cations with low-lying empty atomic orbitals which can overlap with the M–H molecular orbitals of the hydrides in a type of Lewis acid–Lewis base interaction.

There remains the general question as to why the coinage metal cations are particularly suited as 'Lewis acids' for the formation of complexes of the types **$14_{MM'M}$** and **$15_{MM'M}$**. One possible explanation is that the *n*s-orbitals in these cations, being

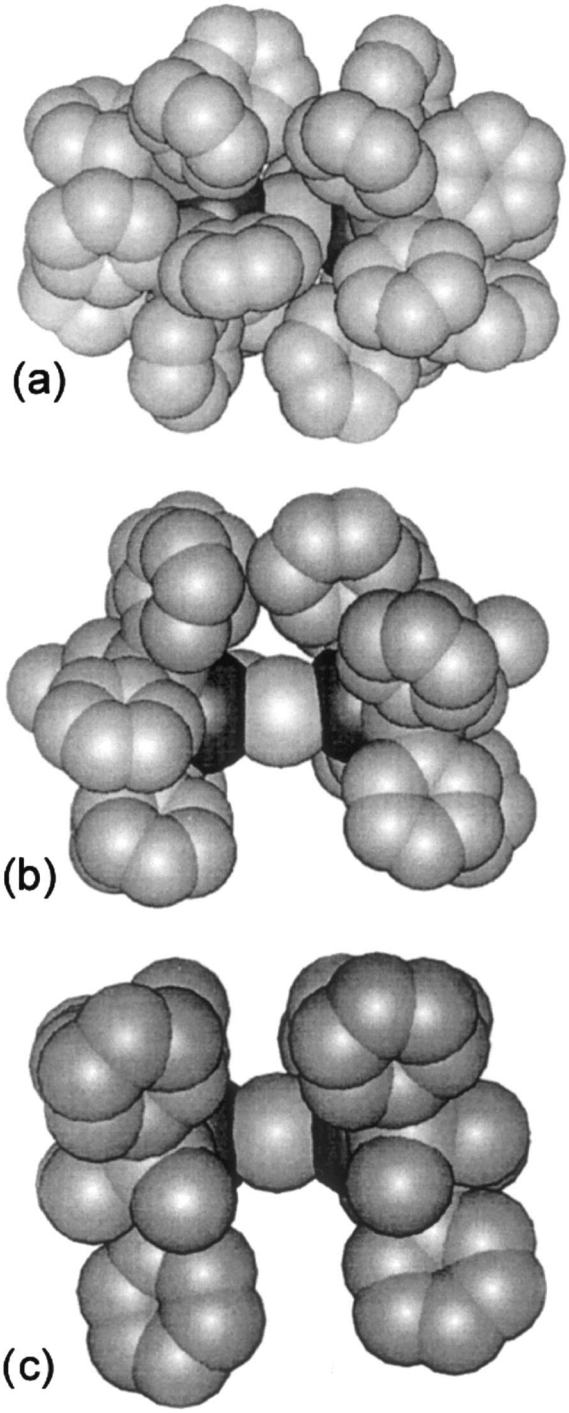

Fig. 9. Space-filling models of the cations in *fac*-[$(PPh_3)_3HIr(\mu\text{-}H)_2Ag(\mu\text{-}H)_2IrH(PPh_3)_3$]($CF_3SO_3$) (**10**) (top (a)), [(triphos)$HIr(\mu\text{-}H)_2Ag(\mu\text{-}H)_2IrH$(triphos)]($CF_3SO_3$) (**$14_{IrAgIr}$**) (middle (b)) and [$(PMe_2Ph)_3HIr$-$(\mu\text{-}H)_2Cu(\mu\text{-}H)_2IrH(PMe_2Ph)_3$][$PF_6$] (**11**) (bottom (c)).

rather diffuse, give a significant overlap with the M–H bonding orbitals, which are also spread over a relatively large surface. There may also be a significant 'ionic' contribution to the overall interaction arising from the positive charge on M′ and the polar and highly polarizable $M^{\delta+}$–$H^{\delta-}$ bonds. Quantitative calculations would require taking into account all these effects.

It is noteworthy that, when the electron affinity of the heterometal becomes too high, an electron-transfer process takes place with decomposition of the trimetallic species. Thus, one finds that when $Hg(CF_3SO_3)_2$ is added to a THF solution of $[IrH_3(triphos)]$ (**18**), in an attempt to obtain $[(triphos)IrH_3HgH_3Ir(triphos)](CF_3SO_3)_2$, precipitation of metallic mercury and formation of $[IrH_2(THF)(triphos)](CF_3SO_3)$ is observed [35].

2.4. Reactivity

In addition to their intrinsic interest, hydrido-bridged heterometallic complexes might be worthy of study as potential catalyst precursors for homogeneously catalyzed reactions. In this context, they would constitute the homogeneous counterparts to the heterogeneous catalysts currently used in a number of important industrial processes [36].

As the most common test reactions in homogeneous catalysis are either C=C or C=O hydrogenation [37], attempts were made to hydrogenate acetone and methyl acrylate, using $[(triphos)RhH_3CuH_3Rh(triphos)]^+$ ($\mathbf{14_{RhCuRh}}$) as a catalyst precursor. No reaction occurred [27]. The observed lack of reactivity may be due to steric factors, i.e. the substrate might have difficulty in reaching the heterometallic center. The space-filling models shown in Fig. 9 support this possibility. Thus, species in which the heterometal is in a less sterically crowded environment would appear to be better candidates as catalyst-precursors for relater hetero-bimetallic organometallic reactions.

3. Bimetallic complexes

As coordinative unsaturation of the coinage metal in the fragment $\{(triphos)MH_3M'\}$ can be compensated with a very low number of ligands (frequent coordination numbers of M′ are 2 and 3), it is conceivable that complexes in which M′ is coordinated to a one or two phosphines, i.e. of the types $[(triphos)MH_3M'(PR_3)_{(n-1)}]^+$ (see Scheme 6) might be obtainable and, possibly, show the desired type of reactivity.

3.1. Monophosphine complexes

Compounds of the type $[(triphos)MH_3M'(PR_3)](CF_3SO_3)$ ($\mathbf{20_{MM'P}}$) and $[(triars)MH_3M'(PR_3)](CF_3SO_3)$ ($\mathbf{21_{MM'P}}$) are obtained only when the phosphine PR_3 is very bulky, e.g. P^tBu_3 (see Scheme 6). The complexes of this type with triphos (M = Rh, Ir; M′ = Cu, Ag) ($\mathbf{20_{MM'P}}$) and triars (M = Rh, Ir; M′ = Cu, Ag) ($\mathbf{21_{MM'P}}$), characterized hitherto are listed in Scheme 6 [27]. They are assigned structures of

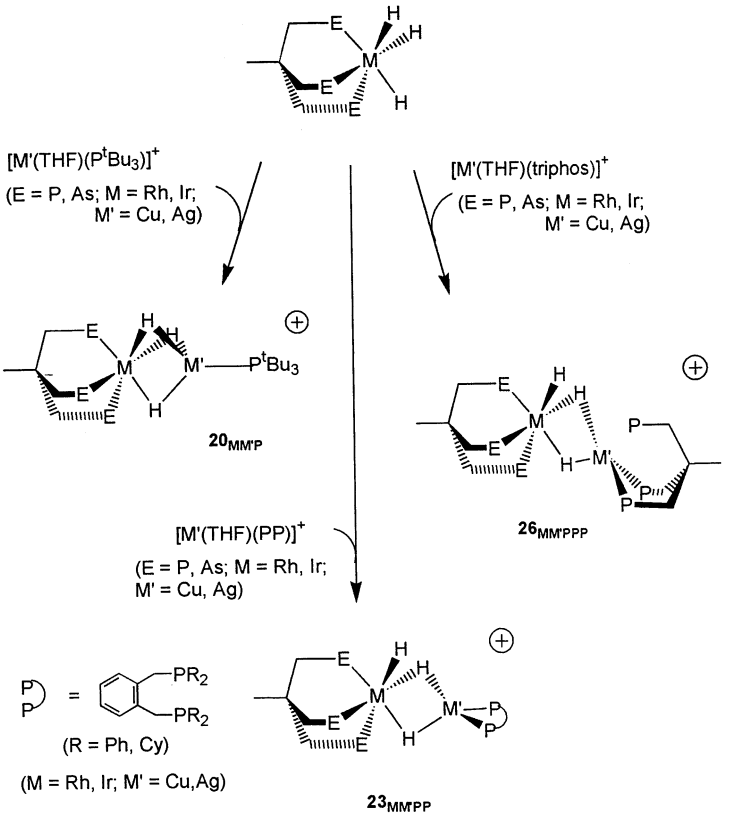

Scheme 6.

the type [(tripod)M(μ-H)$_3$M′(P′Bu$_3$)](CF$_3$SO$_3$) on the basis of their IR spectra which show that all three hydrides are involved in M–H–M′ bridging (see Fig. 10, trace (b)). The ^{1}H- and ^{31}P-NMR spectra are consistent with these structural assignments.

When attempts are made to obtain compounds of the types $\mathbf{20}_{MM'P}$ and $\mathbf{21}_{MM'P}$ using phosphines, which are less bulky than PtBu$_3$, disproportionation of the bimetallic species occurred. The corresponding trimetallic species ($\mathbf{14}_{MM'M}$ and $\mathbf{15}_{MM'M}$, respectively) and the mononuclear complexes [M′(PR$_3$)$_2$](CF$_3$SO$_3$) ($\mathbf{22}_{M'}$) were formed (Eq. (1)) [27]. One can then deduce that the successful isolation of compounds of the types $\mathbf{20}_{MM'P}$ and $\mathbf{21}_{MM'P}$ requires the destabilization of the [M′L$_2$]$^+$ complexes ($\mathbf{20}_{M'}$).

$$2[(\text{triphos})\underset{\mathbf{20}_{MM'P}}{MH_3M'(PR_3)}](CF_3SO_3) \rightleftarrows [(\text{triphos})\underset{\mathbf{14}_{MM'M}}{MH_3M'H_3M}(\text{triphos})](CF_3SO_3) + \underset{\mathbf{22}_{M'}}{[M'(PR_3)_2]}(CF_3SO_3) \quad (1)$$

Given their low stability, $\mathbf{20}_{MM'P}$ and $\mathbf{21}_{MM'P}$ were not tested as heterometallic, homogeneous catalyst precursors.

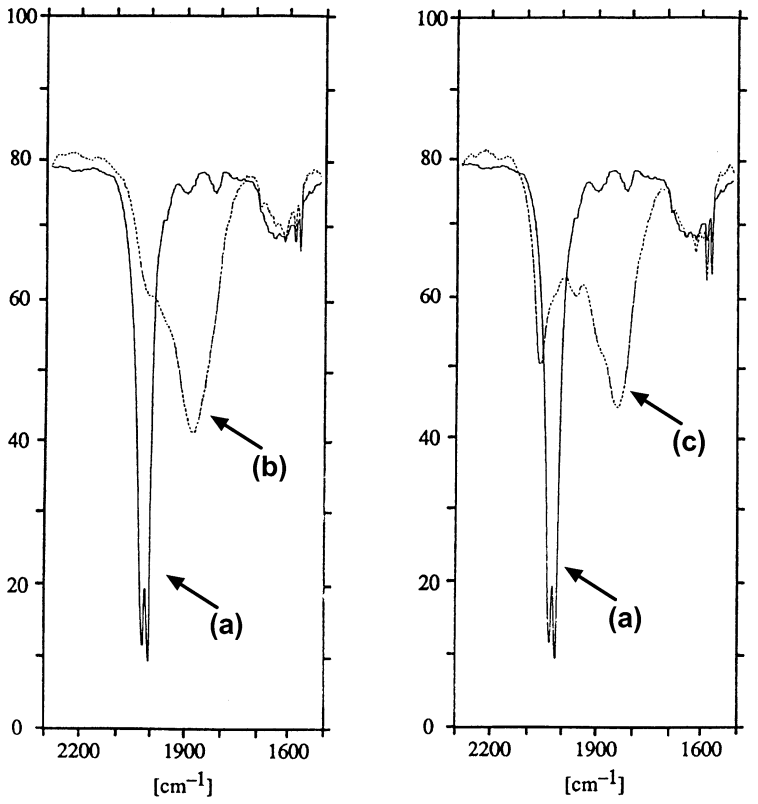

Fig. 10. The IR spectra, in the hydride region of $[IrH_3(triphos)]$ (**18**) (trace (a)) and $[(triphos)Ir(\mu\text{-}H)_3Cu(P^tBu_3)](CF_3SO_3)$ ($\mathbf{20_{IrCuP}}$) (trace (b)) and $[(triphos)HIr(\mu\text{-}H)_2Cu(o\text{-}(Ph_2PCH_2)_2C_6H_4)](CF_3SO_3)$ ($\mathbf{23_{IrCuPP}}$) (trace (c)).

3.2. Bisphosphine complexes

The search for less labile complexes was then directed towards species of the type $[(tripod)MH_3M'(PP)]^+$ (tripod = tripod, PP = bidentate phosphine; M = Rh, Ir; M′ = Cu, Ag, ($\mathbf{23_{MM'PP}}$); triphos = triars, M = Rh, Ir; M′ = Cu, Ag, ($\mathbf{24_{MM'PP}}$). Also these complexes are obtained as shown in Scheme 6 [27] only if bulky bisphosphines such as those shown in the above scheme are used, otherwise ligand disproportionation shown in Eq. (2) occurs.

$$2[(triphos)\underset{\mathbf{23_{MM'PP}}}{MH_3M'(PP)}](CF_3SO_3) \rightleftarrows [(triphos)\underset{\mathbf{14_{MM'M}}}{MH_3M'H_3M}(triphos)](CF_3SO_3) + [M'(PP)_2]\underset{\mathbf{25_{M'}}}{(CF_3SO_3)} \quad (2)$$

Thus, also the formation of complexes of the type $\mathbf{23_{MM'PP}}$ and $\mathbf{24_{MM'PP}}$ require ligands that destabilize the M′-complex of type $\mathbf{25_{M'}}$. The IR spectra of complexes $\mathbf{23_{MM'PP}}$ (see Fig. 10, trace (c)) indicate that the most likely formulation for complexes is $[(triphos)HM(\mu\text{-}H)_2M(PP)]CF_3SO_3$) as a strong terminal M–H band in the region of terminal M–H bonds is present.

Also attempts to use **23**$_{\mathbf{RhCuPP}}$ as catalyst precursor for the homogeneous hydrogenation of methyl acrylate were unsuccessful [27].

3.3. Trisphosphine complexes

Finally, it was of interest to see what compound would be produced when a trihydride of the type [MH_3(tripod)] (M = Rh, Ir; tripod = triphos, triars) is reacted with a cation of the type [M′(THF)(tripod)]$^+$ (M′ = Cu, Ag; tripod = triphos, triars). These reactions gave the compounds [(tripod)MH_3M′(tripod)]CF_3SO_3) (**26**$_{\mathbf{MM'PPP}}$) [27] (see Scheme 6). Their IR spectra in the hydride region are complex: they show a band at ca. 2020 cm^{-1} indicating the presence of terminal Ir–H bonds as well as three bands between 1800 and 1950 cm^{-1}. The formulation given in Scheme 6 is based on the X-ray crystal structure of 'CuH(triphos)' (**27**) which has the structure shown schematically below [38].

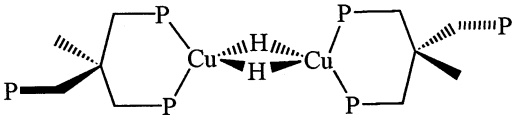

27

3.4. NMR spectroscopy

As can be readily imagined, a great wealth of valuable NMR data can be obtained from these sets of compounds which contain so many NMR active nuclei with spin $S = 1/2$.

Given the complexity of the spectra of most of these compounds, more advanced NMR techniques were employed to obtain the desired parameters. An example of the use of 2D-{^{1}H,^{109}Ag}-inverse correlation spectrum, recorded for [(triars)IrH_3Ag(*o*-(PPh_2CH_2)$_2C_6H_4$)](CF_3SO_3) (**24**$_{\mathbf{IrAgPP}}$), is shown in Fig. 11 [39]. Some data for a selection of silver-containing compounds are given in Table 2 [27]. As can be seen there, the value of ^1J(^{109}Ag,^{1}H) decreases with an increase in the number of phosphorus atoms directly bonded to silver. This decrease is significant (9.9 Hz) when P′Bu_3 in **20**$_{\mathbf{IrAgP}}$ is replaced by the bisphosphine PP in **23**$_{\mathbf{IrAgPP}}$ and is consistent with the postulate that the Ir(μ-H)$_3$-fragment in the former complex becomes an Ir(μ-H)$_2$-bridge in latter species. However, the decrease in ^1J(^{109}Ag,^{1}H) is quite small (0.7 Hz) when the bidentate ligand PP is replaced by triphos as in **26**$_{\mathbf{IrAgPPP}}$. This difference may indicate that there is effectively only an Ir(μ-H)$_2$-bridge also in this complex.

Summing up, on the basis of the IR and NMR spectroscopic data the static structures of the complexes of the above three types can be schematically represented as shown in Scheme 6.

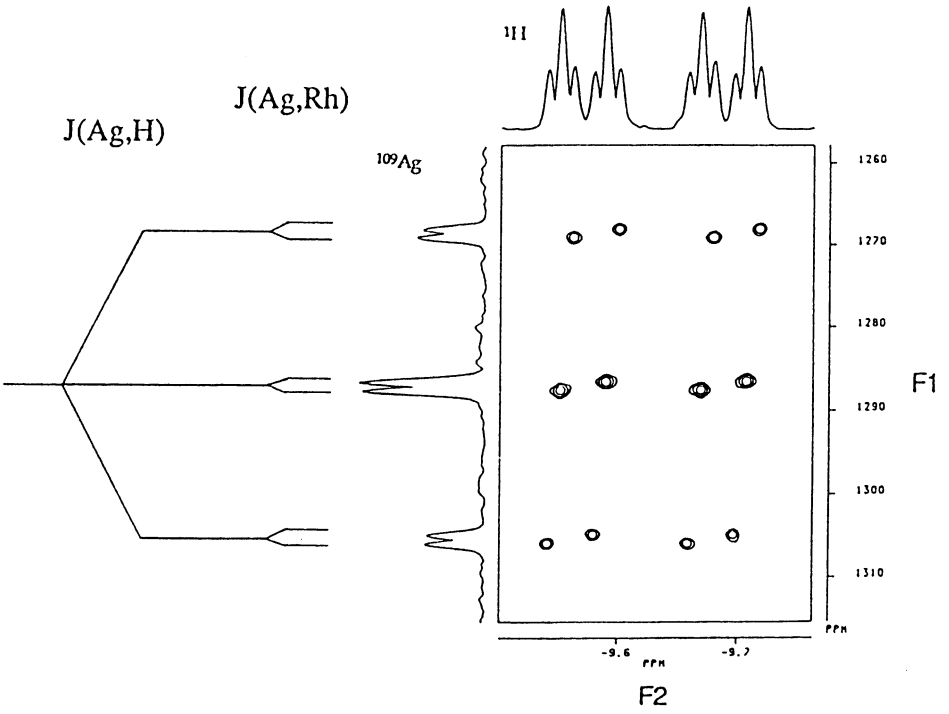

Fig. 11. The 2D-{^{1}H,^{109}Ag}-inverse correlation spectrum of [(triars)HIr(μ-H)$_2$Cu(*o*-(Ph_2PCH_2)$_2C_6H_4$)]-(CF_3SO_3) (**26$_{IrCuPP}$**).

4. Hexametallic complexes

The sets of complexes, in which the ratio of trihydride [MH_3(tripod)] to coinage metal M′ is 1:1 (discussed in an earlier section) were obtained when the reagents were reacted in the presence of one equivalent of an additional phosphine. It was; therefore, of interest to establish which species were formed when the two metal-

Table 2
Some NMR chemical shift values (ppm) and coupling constants (Hz) of the heterobimetallic complexes [(triphos)Ir(μ-H)$_3$Ag(P′Bu_3)](CF_3SO_3) (**20$_{IrAgP}$**), [(triphos)HIr(μ-H)$_2$Ag(*o*-(Ph_2PCH_2)$_2C_6H_4$)](CF_3SO_3) (**23$_{IrAgPP}$**) and [(triphos)$H_{(3-n)}$ Ir(μ-H)$_n$Ag(triphos)](CF_3SO_3) (**26$_{IrAgPPP}$**) [27]

	20$_{IrAgP}$	**23$_{IrAgPP}$**	**26$_{IrAgPPP}$**
δH	−10.63	−10.22	−10.02
δP_{Ir}	−7.28	−9.20	−9.94
δP_{Ag}	86.38	−1.59	−26.89
$^{1}J(^{107}Ag,^{1}H)$	44.6	33.6	34.0
$^{1}J(^{107}Ag,^{31}P)$	536.7	301.1	178.9
$^{4}J(^{31}P_{Ir},^{31}P_{Ag})$	6.9	9.6	7.7

containing reagents were reacted *in the absence* of additional ligands. These conditions led to the formation of the astonishing class of hexametallic clusters $[\{(triphos)MH_3M'\}_3]^{3+}$ (M = Rh, Ir; M′ = Cu, Ag, Au) (**28$_{M3M'3}$**) as shown in Scheme 7 [27,40]. A related complex, $[\{(PMe_2Ph)_3OsH_3Cu\}_3]$, was obtained by Caulton and co-workers [41].

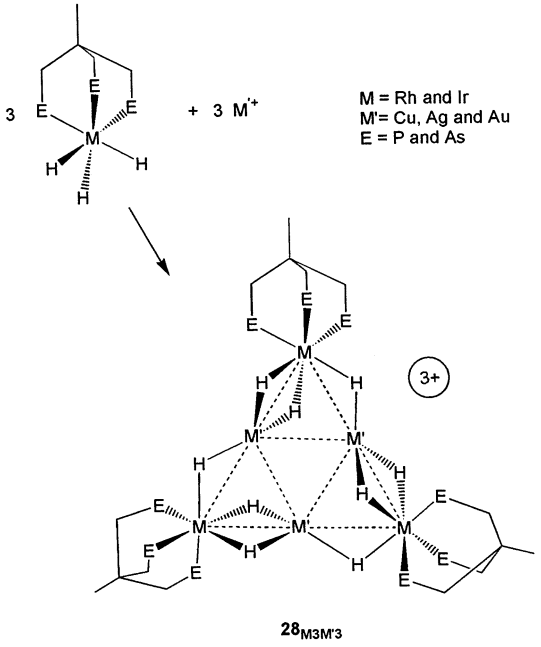

28$_{M3M'3}$

Scheme 7.

X-ray diffraction studies of $[\{(triphos)RhH_3Ag\}_3](CF_3SO_3)_3$ (**28$_{Rh3Ag3}$**) [42] and $[\{(triphos)IrH_3Ag\}_3](CF_3SO_3)_3$ (**28$_{Ir3Ag3}$**) [43] confirm the postulated structures.

Both trications show a striking structural feature: they are shaped like a 'basket' and its 'bottom' consists of the six metal centers, bridged by the nine hydrides. In **28$_{Ir3Ag3}$** one triflate anion is placed 'inside the basket', one of its oxygen atoms (O6) interacting mainly with two silver ions (Ag1 and Ag3) (see Fig. 12). As the shortest Ag–O contacts are ca. 3.0 Å, this interaction appears to be mainly electrostatic in nature.

Another interesting structural feature of compounds **28$_{Rh3Ag3}$** and **28$_{Ir3Ag3}$** is arrangements of the hydrides around the perimeter of the hexametallic core, which consists of a triangle of silver atoms enclosed within a triangle of iridium atoms. Although the hydrides could not be located on the Fourier map, their positions can be inferred from those of the metal and phosphorus atoms. If the three hydrides on, e.g. each iridium are placed using the 'geometrical construction' model described earlier, two of them bridge one of the Ir–Ag edges and the third builds a single bridge spanning the opposite Ir–Ag edge. Thus, there is an alternation of singly and doubly bridged Ir–Ag edges. The Ir–Ag distances listed in Table 3 clearly show this

[41,42]: the shorter Ir–Ag bonds correspond to those where one places two bridging hydrides and the longer Ir–Ag bonds are found where one places one bridging hydride.

The spectroscopic data are in agreement with the above formulation. Thus, the IR spectra of these complexes in the hydride region show only one broad band centered at ca. 1750 cm^{-1} [27]. Also the NMR spectra are consistent with this formulation. Once again, the ^{1}H spectra of the hexametallic cations are quite complex and only the more advanced techniques allow the determination of the relevant parameters.

It would certainly be interesting to study the 'coordinating properties' of anionic ligands with these trications: anions smaller than CF_3SO_3 could fit even better into the cluster cavity and interact much more strongly with the metal atoms inside the cluster. These interactions could change the reactivity of the anions and lead to the formation of unusual products.

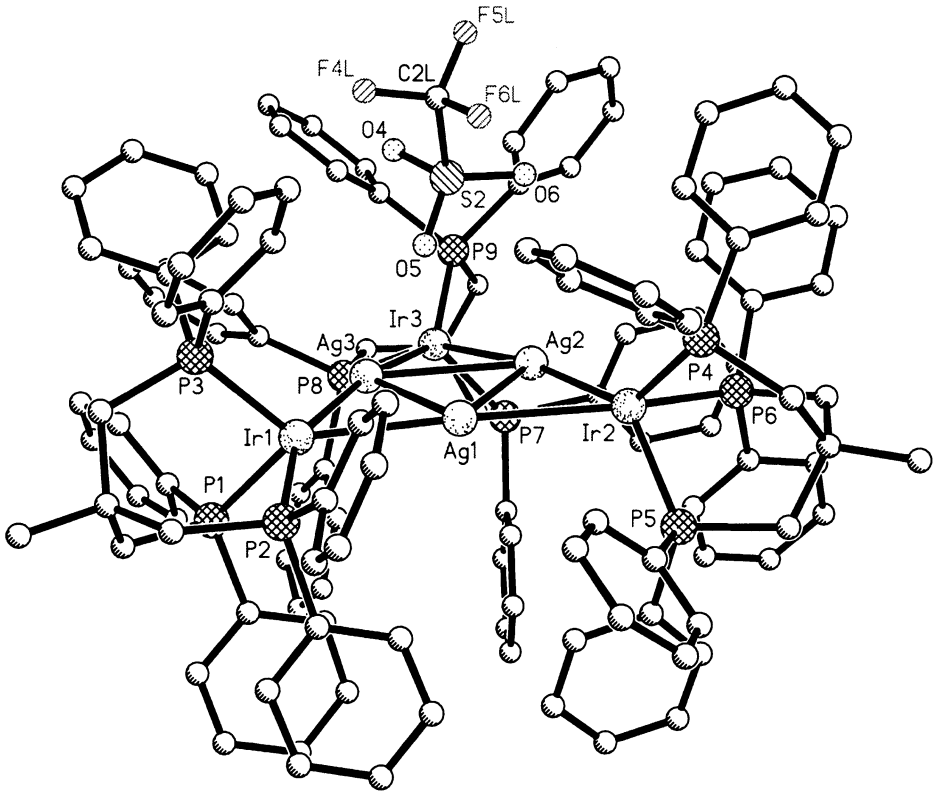

Fig. 12. A view of the interaction between the silver cations and the CF_3SO_3-anion in [{(triphos)HIr(μ-H)$_2$Ag}$_3$$CF_3SO_3$]($CF_3SO_3$)$_2$ (**28$_{Ir3Ag3}$**).

Table 3
A selection of bond lengths (Å) and (°) angles in $[\{(triphos)IrH_3Ag\}_3(CF_3SO_3)](CF_3SO_3)_2$ ($\mathbf{28_{Ir3Ag3}}$)[a]

Bond lengths		Bond angles	
Ir1–Ag1	2.814(1)	Ag1–Ir1–Ag3	61.69(3)
Ir1–Ag3	2.945(1)	Ag1–Ir2–Ag2	62.33(3)
Ir2–Ag1	2.936(1)	Ag2–Ir3–Ag3	62.80(3)
Ir2–Ag2	2.808(1)	Ag1–Ag2–Ag3	59.48(3)
Ir3–Ag2	2.913(1)	Ag2–Ag3–Ag1	60.13(3)
Ir3–Ag3	2.808(1)	Ag3–Ag1–Ag21	60.39(3)
Ag1–O4	5.28(1)	Ir1–Ag3–Ir3	171.47(4)
Ag1–O5	3.08(1)	Ir1–Ag1–Ir2	176.50(4)
Ag1–O6	4.63(1)	Ir2–Ag–2–Ir3	171.68(4)
Ag2–O4	4.54(1)	Ir1–Ag1–Ag3	61.34(3)
Ag2–O5	3.42(1)	Ir1–Ag3–Ag1	56.97(3)
Ag2–O6	3.48(1)	Ir2–Ag1–Ag2	56.72(3)
Ag3–O4	4.05(1)	Ir2–Ag2–Ag1	60.95(3)
Ag3–O5	3.09(1)	Ir3–Ag2–Ag3	56.88(3)
Ag3–O6	4.61(1)	Ir3–Ag3–Ag2	60.32(3)

[a] Displacements (Å) from-least square plane defined by Ir1, Ir2, Ir3: Ag1 = +0.20; Ag2 = +0.20; Ag3 = +0.08. Displacements (Å) from least square plane defined by (a) Ag1, Ag2, Ag3: Ir1 = −0.08; Ir2 = −0.08; Ir3 = −0.32.

5. Conclusions

The coinage metal cations and the trihydrides $[MH_3(triphos)]$, as well as related compounds, can be considered as the building blocks of an albeit restricted LEGO® set: they can be used to build up larger molecular assemblies with interesting structural features. Undoubtedly, much larger metal assemblies could be constructed using elements taken from the types of compounds discussed above. Indeed, a wide range of polymetallic compounds related to those described above [44] have been isolated and characterized, more or less deliberately, although, in most cases, their systematics and reactivities do not appear to have been followed up. The same can almost be said of the compounds described above. However, the authors of this review hope that their contribution will stimulate further work in this area.

Acknowledgements

The authors are greatly indebted to Professor P. Hofmann and Professor U. Röthlisberger for helpful suggestions regarding the bonding in the trimetallic hydrides and to Mr. P. Latal for valuable assistance with the preparation of the figures.

References

[1] (a) D.S. Moore, S.D. Robinson, Chem. Soc. Rev. (1983) 415. (b) K.G. Anderson, Adv. Organomet. Chem. 35 (1993) 1. (c) R.H. Crabtree, Angew. Chem. Int. Ed. Engl. 32 (1993) 789.
[2] (a) J.L. Petersen, L.F. Dahl, J.M. Williams, in: R. Bau (Ed.), Transition Metal Hydrides, Adv. in Chem. Series, No. 167, American Chemical Society, Washington, DC, 1978, p. 11. (b) R.G. Teller, R. Bau, Structure and Bonding, 44 (1980) 1. (c) B. Bau, M.H. Drabnis, Inorg. Chim. Acta 259 (1997) 27.
[3] (a) C.B. Cooper, D.F. Shriver, S. Onaka, in: R. Bau (Ed.), Transition Metal Hydrides, Adv. in Chem. Series, No. 167, American Chemical Society, Washington, DC, 1978, p. 167. (b) J. Rozière, A. Potier, Bull. Chem. Soc. France (1982) 339. (c) I.J. Braid, J. Hoard, J. Tomkinson, J. Chem. Soc. Faraday Trans. (1983) 235.
[4] (a) Z. Liu, X.Y. Hall, Coord. Chem. Rev. 135/136 (1994) 845. (b) B. Jezovska-Trebiatowska, B. Nissen-Sobocinska, J. Organomet. Chem. 322 (1987) 331.
[5] J. Rozière, J.M. Williams, R.P. Stewart, J.L. Petersen, L.F. Dahl, J. Am. Chem. Soc. 99 (1977) 4497.
[6] A. Albinati, T.J. Emge, T.F. Koetzle, S.V. Meille, A. Musco, L.M. Venanzi, Inorg. Chem. 25 (1986) 4812.
[7] R.A. Jones, G. Wilkinson, I.J. Colquohon, W. McFarlane, A.M.R. Galas, M.B. Hursthouse, J. Chem. Soc. Dalton Trans. (1980) 2480.
[8] R. Bau, W.E. Carroll, R.G. Teller, T.F. Koetzle, J. Am. Chem. Soc. 99 (1977) 3872.
[9] M.L.H. Green, J.A. McCleverty, L. Pratt, G. Wilkinson, J. Chem. Soc. (1961) 4854.
[10] A. Albinati, A. Togni, L.M. Venanzi, Organometallics 5 (1986) 1785.
[11] A. Albinati, S. Chaloupka, J. Eckert, L.M. Venanzi, M.K. Wolfer, Inorg. Chim. Acta 259 (1997) 305.
[12] (a) B.T.M. Willis, Chemical Applications of Thermal Neutron Scattering, Oxford University Press, London, 1972. (b) R.E. Lechner, C. Riekel, Applications of neutron scattering in chemistry, Springer Tracts in Modern Physics, vol. 101, Springer-Verlag, Berlin, 1983.
[13] L.F. Rhodes, J.C. Huffman, K.G. Caulton, J. Am. Chem. Soc. 105 (1983) 5137.
[14] H. Lehner, Dissertation ETH Zürich No. 7239, 1983.
[15] L.F. Rhodes, J.C. Huffman, K.G. Caulton, J. Am. Chem. Soc. 1067 (1984) 6874.
[16] J. Chatt, R.S. Coffey, B.L. Shaw, J. Chem. Soc. (1965) 7391.
[17] P.N. Janser, Dissertation ETH Zürich No. 8790, 1989.
[18] F. Bachechi, J. Organomet. Chem. 474 (1994) 191.
[19] A. Albinati, F. Rominer, unpublished data.
[20] A.G. Orpen, J. Chem. Soc. Dalton Trans. (1980) 2509.
[21] A. Albinati, S. Chaloupka, A. Curao, W.T. Klooster, T.F. Koetzle, R, Nesper, L.M. Venanzi, Inorg. Chim. Acta 300–303 (2000) 903.
[22] S. Chaloupka, L.M. Venanzi, unpublished data.
[23] A. Albinati, J. Eckert, L.M. Venanzi, unpublished data.
[24] A.D. Taylor, E.J. Wood, J.A. Goldstone, J. Eckert, Nucl. Instr. Methods 221 (1984) 308.
[25] D. Graham, Ph.D. Thesis, University of Durham, Durham, UK, 1980.
[26] H. Ruegger, S. Chaloupka, L.M. Venanzi, unpublished data.
[27] U.L. Stadler, Dissertation ETH Zürich No. 9067, 1989.
[28] J. Ott, C.A. Ghilardi, S. Midollini, A. Orlandini, J. Organomet. Chem. 291 (1985) 89.
[29] P. Janser, L.M. Venanzi, F. Bachechi, J. Organomet. Chem. 296 (1985) 229.
[30] F. Bachechi, C. Bianchini, A. Meli, Inorg. Chim. Acta 213 (1993) 269.
[31] A. Albinati, S. Chaloupka, L.M. Venanzi, unpublished data.
[32] T. Albright, J.K. Burdett, M.-H. Whangbo, Orbital Interactions in Chemistry, Wiley, New York, 1980.
[33] C.E. Moore, Atomic Energy Levels, National Bureau of Standards, Circular 467, Washington, DC, 1952 and 1958.

[34] P. Pyykkö, Relativistic theory of atoms and molecules, in: Lecture Notes in Chemistry, vol. 41, Springer-Verlag, Berlin, 1986.
[35] M.K. Wolfer, Dissertation ETH Zürich No. 8151, 1986.
[36] M. Bartok, Stereochemistry of Heterogeneous Metal Catalysis, Wiley, Chichester, 1985.
[37] J.P. Collman, L.S. Hegedus, J.R. Norton, R.G. Finke, Principles and Applications of Organotransition Metal Chemistry, University Science Books, Mill Valley, CA, 1987.
[38] G.V. Goeden, J.C. Huffman, K.G. Caulton, Inorg. Chem. 25 (1986) 2484.
[39] D. Nanz, Dissertation University of Zürich, 1993.
[40] J. Ott, Dissertation ETH Zürich No. 8000, 1986.
[41] T.H. Lemmen, J.C. Huffman, K.G. Caulton, Angew. Chem. 98 (1986) 267.
[42] F. Bachechi, J. Ott, L.M. Venanzi, J. Am. Chem. Soc. 107 (1985) 1760.
[43] S. Chaloupka, R. Nesper, L.M. Venanzi, M. Wörle, unpublished results.
[44] D.M.P. Mingos, D.J. Wales, Introduction to Cluster Chemistry, Prentice-Hall, Englewood Cliffs, NJ, 1990.